ELSEVIER

Journal of Nuclear Materials 307–311 (2002) 1305–1309

journal of nuclear materials

www.elsevier.com/locate/jnucmat

Macroscopic properties and microstructure changes of heavily neutron-irradiated β-Si_3N_4 by annealing

Masafumi Akiyoshi [a,*], Kohki Ichikawa [a], Takako Donomae [b], Toyohiko Yano [a]

[a] *Research Laboratory for Nuclear Reactors, Tokyo Institute of Technology, 2-12-1 O-okayama, Meguro-ku, Tokyo 152-8550, Japan*

[b] *O-arai Engineering Center, Japan Nuclear Cycle Development Institute, Narita-cho, O-arai, Higashi-Ibaragi 311-1393, Japan*

Abstract

Swelling and thermal diffusivity measurements have been carried out on sintered β-Si_3N_4 specimens that were heavily neutron-irradiated in an experimental fast reactor under various conditions. Changes in these parameters after post-irradiation isochronal annealing up to 1500 °C were measured. TEM observation showed that interstitial dislocation loops were formed in many specimens, and were stable after annealing at 1500 °C. Bubbles were formed in the specimens annealed at 1500 °C. Neutron-irradiated β-Si_3N_4 showed small swelling that was recovered very slightly due to annealing up to 1300 °C. The specimens showed very small expansion at 1200–1300 °C, which would be caused by He or H_2 bubble formation. Recovery of the thermal diffusivity is higher in the specimen that did not contain many dislocation loops. The annealing behavior of the thermal diffusivity and macroscopic length in β-Si_3N_4 indicated that interstitial atoms are mobile at least at 380 °C, and vacancies begin to move around 1100 °C.

1. Introduction

Silicon nitride (β-Si_3N_4) is one of the candidate materials for the first-wall in fusion reactors, where it would be exposed to high fluences of 14 MeV fusion neutrons at temperatures up to about 1000 °C [1–7].

High-energy neutron irradiation induces several types of crystalline defects to ceramic materials. At first, knock-on cascades leave Frenkel pairs and other point-like defects. These point or point-like defects are immobile at lower temperature. But at higher temperature, they can move around and aggregate each other to grow dislocation loops or voids. On the other hand, neutron irradiation causes nuclear transmutation. If some atoms are transmuted to gas atoms, they will migrate to form bubbles. Macroscopic volume change is influenced by the amount and type of all these defects, otherwise the thermal diffusivity is reflected mainly by the density of point defects, especially sensitive to vacancies. TEM observations show the distribution of defect aggregates directly, and careful HREM observations enable us to obtain the defect structure, while point defects are invisible.

We already reported the physical property change of heavily neutron-irradiated β-Si_3N_4 and β-SiC by thermal annealing [8]. The irradiation behavior of these materials up to very high doses is still limited, particularly of Si_3N_4. In this paper, therefore we will present additional data on β-Si_3N_4 that was irradiated under different conditions than in the previous report [8].

2. Experimental procedure

The β-Si_3N_4 specimen was manufactured by the Nippon Steel Co. (designated product NS101) from the raw materials of β-Si_3N_4 powder (98.5% purity), together with sintering additives of <10 wt%. of Y_2O_3 (99.9%) and <2 wt%. of $ZrSi_2$ (99%). These materials were sintered by the hot-pressing method, resulting in

* Corresponding author. Tel.: +81-3 5734 3380; fax: +81-3 5374 2959.

0022-3115/02/$ - see front matter
PII: S0022-3115(02)01301-6

almost full density (3.33 g/cm^3). X-ray diffractometry confirmed that the Si_3N_4 phase was dominantly β type.

The dimensions of the specimens were $1.2 \times 1.2 \times 15.5$ mm^3 for swelling measurement, 10 mm in diameter and 2 mm in thickness for thermal diffusivity measurement and 3 mm in diameter and 0.5 mm in thickness for TEM observation, respectively. Neutron irradiation was performed in the experimental fast reactor JOYO in Japan using the irradiation rig CMIR-4. The irradiation conditions for the specimens of swelling and thermal diffusivity measurement are listed in Table 1 and 2, respectively, where the specimens labeled as T61, T65, T72 and T73 were reported in the previous paper [8] and were indicated with asterisks. It is noted that the neutron fluence of specimens for thermal diffusivity measurements was much less than for the other specimens. The irradiation conditions of the specimens for TEM observation were 2.8×10^{26} n/m^2 at 520 °C designated as T51 specimen, 3.9×10^{26} n/m^2 at 620 °C (T53) and 3.7×10^{26} n/m^2 at 727 °C (T57), respectively.

The measurement of macroscopic swelling was performed by a conventional point-type micrometer, and the measurement of the thermal diffusivity was performed by the laser flash method (Rigaku, LF/TCM-FA8510B). Isochronal annealing was conducted every 100 °C up to 1500 °C in a vacuum of $\simeq$1 Pa ($\leqslant$1000 °C) or $\simeq 10^{-4}$ Pa (1100–1500 °C). The samples were annealed for 1 h at an objective temperature. After annealing, each measurement was performed at room temperature.

Foils for electron microscopy were prepared by the Ar ion-beam milling method after irradiation. The transmission electron microscope used in this study was an H-9000 (Hitachi, Japan) and was operated at an accelerating voltage of 300 kV.

Table 1
Results of swelling measurements and their irradiation conditions

Specimen ID	Fluence (n/m^2) ($E > 0.1$ MeV)	Temperature (°C)	Length change (linear %)
∗T61	2.8×10^{26}	482	+0.19
T63	3.9×10^{26}	585	+0.36
∗T65	4.2×10^{26}	731	+0.23
T67	3.7×10^{26}	735	+0.16

3. Results

The macroscopic length change of as-irradiated specimens is shown in Table 1. The T63 specimen showed relatively large swelling compared to the other specimens, but it is, absolutely still very small, 0.36%. Table 2 indicates that the thermal diffusivity change of the as-irradiated specimen mostly depended on the irradiation temperature. The neutron-irradiation fluence of the T72 specimen was three times as much as that of the T71 specimen, but the former specimen kept a little higher thermal diffusivity than the latter specimen, because the irradiation temperature of the T72 specimen (394 °C) was slightly higher than that of the T71 specimen (377 °C). Furthermore, the irradiation temperature of the T73 specimen (542 °C) was fairly higher than those of the other specimens, so the thermal diffusivity of the T73 specimen kept a fairly high value, 0.0717 cm^2/s corresponding to a 71.3% decrease from the value of the unirradiated specimen.

Fig. 1 shows the change in macroscopic length as a function of annealing temperature. Macroscopic lengths of all specimens decreased gradually from the irradiation temperature until to about 1100 °C. After annealing above 1300 °C, all specimens showed large shrinkage. All specimens became shorter than that of before irradiation after annealing at 1500 °C. This large shrinkage

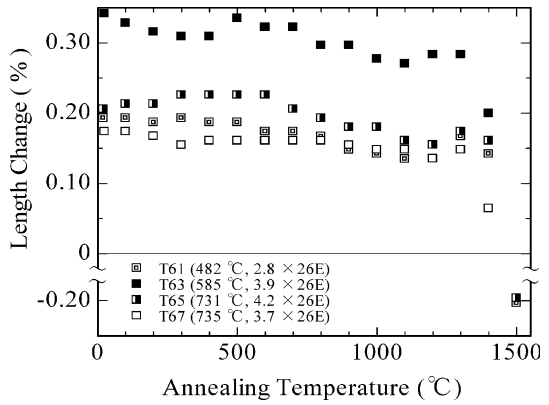

Fig. 1. Recovery of macroscopic length change in β-Si_3N_4 irradiated under various conditions as a function of annealing temperature.

Table 2
Results of thermal diffusivity measurements and their irradiation conditions

Specimen ID	Fluence (n/m^2) ($E > 0.1$ MeV)	Temperature (°C)	Thermal Diffusivity		
			Unirradiated (cm^2/s)	Irradiated (cm^2/s)	Change (%)
T71	0.5×10^{26}	377	–	0.0400	−84.0
∗T72	1.4×10^{26}	394	0.250	0.0478	−80.9
∗T73	0.4×10^{26}	542	–	0.0717	−71.3

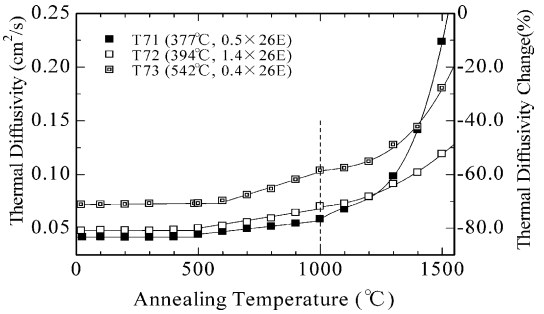

Fig. 2. Recovery of thermal diffusivity in β-Si_3N_4 irradiated under various conditions as a function of annealing temperature.

was also observed in the unirradiated specimen. In addition, all specimens show a very small expansion around 1200–1300 °C.

Changes in thermal diffusivity as a function of annealing temperature is given in Fig. 2. All specimens show that the recovery curves have two stages. In the first stage, the recovery starts around the irradiation temperature, and the recovery curve can be fitted to a linear function. The second stage starts above 1000 °C and the recovery curve can be fitted to a quadratic or cubic function. After annealing up to 1500 °C, the T71 specimen leaves a small decline (11%) in thermal diffusivity, and the T72 and T73 specimens leave 52% and 28% decline, respectively.

Fig. 3 shows the HREM image of β-Si_3N_4 after annealing up to 1500 °C (T61 specimen). The irradiation condition of this specimen was almost the same as the T51 specimen, and the HREM image of the T51 specimen without annealing showed mostly the same defect type (interstitial dislocation loop [9,10]), size and concentration as in Fig. 3. In addition, the T63, T65, and T67 specimens showed the same tendency before and

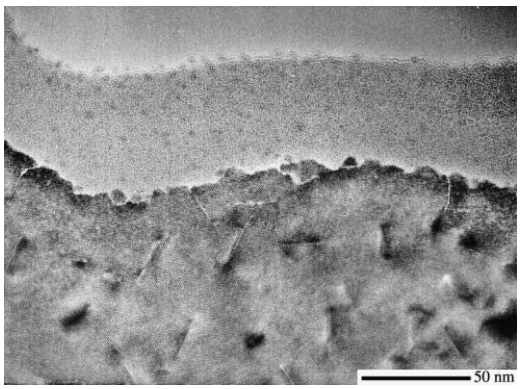

Fig. 3. A HREM image of neutron-irradiated β-Si_3N_4 (T61) after annealing up to 1500 °C.

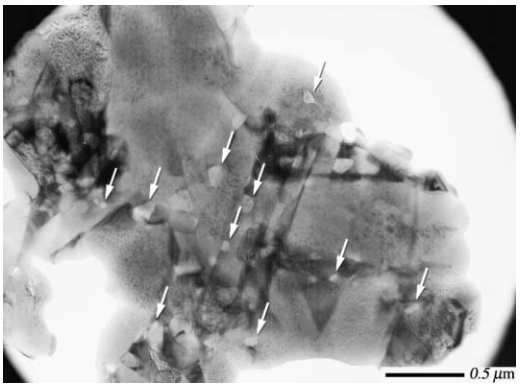

Fig. 4. A bright field image of neutron-irradiated β-Si_3N_4 (T65) after annealing up to 1500 °C. White arrows indicate bubbles.

after annealing, the specimens showed resemble size and concentration of defects. Fig. 4 shows a bright-field image of the T65 specimen after annealing up to 1500 °C. Some bubbles, indicated by white arrows, are observed along grain boundary of the sintered body. The other specimens, T61, T63, T67, after annealing up to 1500 °C showed a similar bubble structure.

4. Discussion

The β-Si_3N_4 powder was reported to decompose about 5 wt%. by heating at 1510 °C for 1 h in vacuum [11]. A bulk specimen for macroscopic length measurements is more stable than powder because the nitrogen gas diffusion in the specimen requires a higher activation energy than that of decomposition [12]. So, linear shrinkage of ≃0.5% above 1400 °C in Fig. 1 can be attributed to the pyrolysis of β-Si_3N_4 due to annealing in vacuum.

The very small expansion around 1200–1300 °C in Fig. 1 is expected to be caused by H_2 or He bubbles. Fig. 4 shows some bubbles which were created in the specimen annealed up to 1500 °C, while these bubbles were not found in the as-irradiated specimens. H_2 or He is considered to be created by nuclear transmutation reactions ${}_7{}^{14}N$ (n, p) ${}_6{}^{14}C$ or ${}_7{}^{14}N$ (n, α) ${}_5{}^{11}B$. The amounts of He and H were expected to have almost the same concentration (≃200 appm) based on calculations using the JENDL-Gas Production Library, 1991. Many hydrogen atoms should migrate and go out of the specimen, but some of them were trapped at vacancies to form bubbles. In the case of He, bubbles may be formed.

Low magnification TEM observations and HREM observations showed that neutron-induced dislocation loops did not diminish after 1500 °C annealing. Growth of dislocations was not confirmed. These dislocation loops were classified into some types, and two types of them were analyzed and structure models were

obtained [9,10]. Each model was created by rearrangement of SiN_4 tetrahedra. In the type-I structure, one SiN_4 tetrahedral layer was inserted into {1 0 0} planes, and in the type-II structure, it was inserted into {1 1 0} planes. Both planes consist of three symmetrically equivalent planes. All these planes are perpendicular to the hexagonal (0 0 1) plane and cross each other, but type-I or type-II dislocations forbid to cross the same type or the other type dislocations. Once that dislocation loops were formed very closely and adjoin each other they confine further growth of the dislocation loops. Vacancies and interstitials lose their sink, and annihilate each other, so that macroscopic swelling is restrained. Other factors on swelling such as an effect of an oxide secondary phase are not eliminated.

The recovery curve of thermal diffusivity may indicate the threshold temperature on which interstitial atoms begin to move. The first stage of recovery mainly caused by migration of interstitial atoms. Pay attention to the recovery curve of the T71 specimen in Fig. 2. As-irradiated specimens show relatively low thermal diffusivity because of low irradiation temperature, where the recombination radius is not so large and many point defects remain in the specimen. The thermal diffusivity started to recover from almost irradiation temperature. This phenomenon can be explained by migration of interstitials, resulting the annihilation of vacancies. But once that interstitial atoms form small clusters, it will require a higher temperature to migrate. The first stage of recovery may reflect these various energy states of interstitial atoms. In other words, a part of interstitials are mobile at least at the irradiation temperature of the T71 specimen, the lowest irradiation temperature specimen. The recovery of the macroscopic length of all specimens was also observed after the annealing above the irradiation temperature. This is also attributed to the annihilation of point-like defects by migration of interstitials.

Next, pay attention to the recovery curves of the T71 and T72 or T73 specimens. The thermal diffusivity of the as-irradiated specimens increases with irradiation temperature. But, after annealing up to 1500 °C, the T73 specimen shows smaller recovery than that of T71. The T72 specimen shows very small recovery and leaves 50% of decline. These results are explained as follows. Interstitial atoms begin to move and create interstitial dislocation loops during irradiation around the irradiation temperature of the T71 specimen (377 °C) and the T72 specimen (394 °C). Once that interstitial atoms migrate into dislocation loops, they will not work as a vacancy sink any longer. At the irradiation temperature of the T71 specimen, very few interstitial dislocation loops were created because the temperature and fluence were very close to the threshold of the growth of the loop, and it just began to nucleate. At higher temperature, the amount of these dislocation loops may increase with irradiation dose, and it corresponds to the amount of decline of the thermal diffusivity after annealing. So the T72 specimen (1.4×10^{26} n/m^2 ($E > 0.1$ MeV)) leaves a larger decline than that of T73 (0.4×10^{26} n/m^2). Further microscopic observations should be necessary to confirm this estimation.

From Fig. 1, the macroscopic length increases slightly above 1100 °C. This seems to be caused by bubble formation as observed in Fig. 4. The bubble formation is accelerated by vacancy migration. Thus, it is concluded that the vacancies will be mobile at around 1100 °C in β-Si_3N_4. The change in recovery curves of the thermal diffusivity for all specimens at around 1100 °C may correspond to the migration of vacancies, but further examinations are necessary to confirm the mechanism.

5. Conclusion

Swelling and thermal diffusivity measurements and TEM observations have been carried out on heavily neutron-irradiated β-Si_3N_4. The changes were measured after post-irradiation isochronal annealing up to 1500 °C. Neutron-irradiated β-Si_3N_4 showed small swelling that was recovered slightly due to annealing up to 1300 °C. All specimens show very small expansion at 1200–1300 °C. In addition, after annealing at 1400-1500 °C, all specimens showed large shrinkage because of the pyrolysis of β-Si_3N_4 in vacuum. TEM observations showed that bubbles were formed after annealing up to 1500 °C, and these are considered to be He or H_2 bubbles created by transmutation. The HREM observation found out the occurrence of interstitial dislocation loops, which were stable up to 1500 °C. The annealing behavior of the thermal diffusivity and macroscopic length indicated that interstitial atoms are mobile at least at 380 °C, and vacancies begin to move around 1100 °C.

Acknowledgements

The neutron-irradiated specimens were kindly supplied by the Japan Nuclear Cycle Development Institute under the contract between Tokyo Institute of Technology and JNC. The work was also partly supported by the Grant-in-Aids for Scientific Research from the Ministry of Education, Science, Sports and Culture, Japan.

References

[1] L.H. Rovner, G.R. Hopkins, Nucl. Technol. 29 (1976) 274.
[2] F.W. Clinard Jr., G.F. Hurley, R.W. Klaffky, Res. Mech. 8 (1983) 207.

[3] G.P. Pells, J. Nucl. Mater. 122&123 (1984) 1338.
[4] F.W. Clinard Jr., G.F. Hurley, L.W. Hobbs, D.L. Rohv, R.A. Youngman, J. Nucl. Mater. 122&123 (1984) 1386.
[5] G.R. Hopkins, R.J. Price, Nucl. Eng. Design/Fus. 2 (1985) 111.
[6] Y.Y. Liu, D.L. Smith, J. Nucl. Mater. 141–143 (1986) 38.
[7] C. Kinoshita, S. Zinkle, J. Nucl. Mater. 233–237 (1996) 100.
[8] T. Yano, M. Akiyoshi, K. Ichikawa, Y. Tachi, Y. Iseki, J. Nucl. Mater. 289 (2001) 102.
[9] M. Akiyoshi, T. Yano, M. Jenkins, Philos. Mag. A 81 (2001) 683.
[10] M. Akiyoshi, T. Yano, M. Jenkins, Philos. Mag. Lett 81 (2001) 251.
[11] H. Suzuki (Ed.), High Temperature Ceramics Materials, Nikkankougyousinbun-shya, 1985.
[12] H.D. Batha, E.D. Whitney, J. Am. Ceram. Soc. 56 (1973) 365.